Journal of Innovative Optical Health Sciences
Vol. 9, No. 3 (2016) 1630009 (11 pages)

DOI: 10.1142/S1793545816300093

World Scientific
www.worldscientific.com

Extending the spatiotemporal resolution of super-resolution microscopies using photomodulatable fluorescent proteins

Mingshu Zhang*,†, Zhifei Fu*,†,‡ and Pingyong Xu*,†,§
*Key Laboratory of RNA Biology, Institute of Biophysics
Chinese Academy of Sciences Beijing, 100101, P.R. China
†Beijing Key Laboratory of Noncoding RNA
Institute of Biophysics
Chinese Academy of Sciences, Beijing, 100101, P.R. China
‡Graduate School of the Chinese Academy of Sciences
Beijing, P.R. China
§pyxu@ibp.ac.cn

Received 14 March 2016
Accepted 18 April 2016
Published 17 May 2016

In the past two decades, various super-resolution (SR) microscopy techniques have been developed to break the diffraction limit using subdiffraction excitation to spatially modulate the fluorescence emission. Photomodulatable fluorescent proteins (FPs) can be activated by light of specific wavelengths to produce either stochastic or patterned subdiffraction excitation, resulting in improved optical resolution. In this review, we focus on the recently developed photomodulatable FPs or commonly used SR microscopies and discuss the concepts and strategies for optimizing and selecting the biochemical and photophysical properties of PMFPs to improve the spatiotemporal resolution of SR techniques, especially time-lapse live-cell SR techniques.

Keywords: Super-resolution; PMFP; mGeos; mEos3; Skylan-S; Skylan-NS.

1. Introduction

Fluorescence microscopy using genetically encoded fluorescent proteins (FPs) plays a key role in elucidating biological processes as well as *in vivo* dynamics in a minimally invasive manner. However, because of the diffraction limit, it is a challenge to visualize objects with sizes smaller than 200 nm in the lateral direction and 500 nm in the axial direction. To overcome this problem, several super-resolution (SR) techniques have been developed to extend the diffraction-limited spatial resolution by as much as an order of magnitude.[1–7] Most of these

§Corresponding author.

SR techniques use light-controllable FPs whose fluorescence emission is modulated by light irradiation with specific wavelengths. We refer to these light-controllable FPs as photomodulatable FPs (PMFPs). Compared with organic dyes, FPs enable easy and genetically specific labeling of both fixed and living cells. Although some unique characteristics of organic dyes and other fluorophores, such as their brightness and photostability, can be superior to those of PMFPs, the sophisticated approaches required to deliver them into biological cells and to decrease unspecific labeling limit their application mainly to fixed samples and make the imaging of living cells a challenge. There are three classes of PMFPs: photoactivatable FPs (PAFPs), photoconvertible (also called photoswitchable) FPs (PCFPs), and reversibly photoswitchable FPs (RSFPs).[8,9] PAFPs can be activated from a nonfluorescent (dark) state to a fluorescent state, whereas PCFPs undergo a conversion from one color to another. In contrast to PAFPs and PCFPs, RSFPs can be reversibly photoswitched between the active and inactive states. In this review, we focus on the recently developed PMFPs for commonly used SR microscopies and discuss the concepts and strategies for optimizing and choosing the biochemical and photophysical properties of PMFPs to enhance the spatiotemporal resolution of SR techniques, especially time-lapse live-cell SR imaging.

2. Breaking the Diffraction Limit with Photomodulatable FPs

The image of an infinitely small object under a light microscope consists of a central spot surrounded by a series of higher-order diffraction rings. The size of the central spot (also called the Airy disk) is equal to the diffraction limit, d, which is given by the equation $d = 0.61\,\lambda/\mathrm{NA}$, where λ is the emission wavelength and NA is the numerical aperture of the objective.[10] Fluorophores within the diffraction limit remain indiscernible from each other if their fluorescent signals are simultaneously recorded. In the past decades, several SR techniques have been developed to break the diffraction limit. The main principle of these techniques is to prevent the simultaneous excitation or emission of all the fluorophores in the sample using nonuniform subdiffraction excitation or emission within the diffraction spot, successively changing the excitation or emission location and recording time-sequential images. If digital cameras are used, the image within one diffraction-limited zone occupies several pixels. The subdiffraction excitation or emission locations are sequentially moved across the image field to ensure that all the fluorescent molecules within one diffraction-limited zone will be recorded. The time-sequential information on the camera pixels, either the intensity and/or fluctuation of each pixel or the centroid of the single-molecule fluorescent distribution, is used to reconstruct an SR image using different algorithms in different SR techniques. We refer the readers to the recent excellent reviews for in-depth descriptions of these techniques.[11–13]

Generally, there are two strategies of nonuniform subdiffraction excitation or emission: the stochastic emission or the patterned excitation. The first strategy uses PMSFs whose emissions are stochastically controlled by the illumination light so that one, several or an ensemble of molecules within one diffraction-limited zone are recorded at a time. The (f)PALM/STORM[1–3] and single-molecule-based variations[14–17] utilize this strategy to improve resolution by localizing the position(s) of a single fluorophore molecule or overlapping fluorophores, respectively, whereas the super-resolution optical fluctuation imaging (SOFI) technique[18] uses the intensity fluctuation of pixels resulting from the capture of sequential images for a cross-correlation analysis and the SR reconstruction. The second strategy, used in stimulated emission depletion (STED),[7] ground state depletion (GSD) microscopy[19] and structured illumination microscopy (SIM)[6] SR microscopies, relies on the patterned subdiffraction excitation (point pattern or line pattern) to reduce the size of an ensemble of excited fluorophores. During the imaging of the subdiffraction pools at each time point, the signal from the molecules outside of the subdiffraction area in the diffraction-limited area will contribute to the background and signal noise and decrease the resolution. Thus, the near-field scanning optical microscopy (NSOM)[20] that also uses this strategy has a smaller excitation spot size and a lower surrounding fluorescence background within one diffraction-limited zone compared with other SR techniques. Both conventional FPs, such as GFP, and PMFPs can be used for this strategy. However, PMFPs require orders of magnitude lower light intensity by using nonlinear subdiffraction excitation[5,7] and further improve spatial resolution in

saturation-based SR techniques (NL-SIM[21] and RESOLFT[4]). Notably, our recently developed PSFP Skylan-NS and patterned activation NL-SIM (PA NL-SIM) make possible practical noninvasive time-lapse live-cell imaging with very high spatiotemporal resolution.[22]

For both strategies and their related SR techniques, three key characteristics to be discussed later are very important for improving the spatiotemporal resolution: (1) the size of the subdiffraction excitation pattern (spot or line), (2) the fluorescence signal of the subfocus location, and (3) the signal-to-background ratio (SBR). We will focus on recently developed PMSFs and discuss their photochemical properties that are related to resolution improvement in commonly used SR techniques, especially live-cell SR techniques.

3. Photophysical and Biochemical Properties of Photomodulatable FPs

Since the discovery of PMFPs, extensive efforts have been made to engineer FPs with improved properties, with the aim of achieving better image accuracy and precision. The following are some basic properties that determine whether an FP is suitable for use in SR microscopy.

3.1. *Monomeric properties*

This property is very important but often overlooked in SR techniques. In our opinion, it should be the first consideration when choosing an appropriate PMFP for SR imaging as it is not useful to obtain the wrong information from the mislocated artificial structures even if the resolution is extremely high. For a fluorescent protein, it is worth noting that its oligomeric state depends on the concentration, which is related to the local environment in living cells. Many "monomeric" FPs tested in solution or by gel electrophoresis *in vitro* are not as monomeric as they were expected to be and form oligomers once they are confined in a crowded *in vivo* environment such as a membrane. An elevated local concentration of the FPs is the main cause as sedimentation velocity experiments show that FPs that are not true monomers gradually form dimers and higher-order oligomers with increased concentration *in vitro*.[23]

For any SR technique, although different target proteins have different expression levels and intrinsic oligomerization tendencies, a monomeric PMFP should be chosen to minimize the risk of disturbing the localization and function of the target protein. Notably, dimeric FPs may cause artificial clusters of the target proteins by enhancing the dimerization tendency of the target protein.[24] Studies by our group and others show that the oligomerization of FPs affects the target protein localization and even function.[23,24] Fortunately, many truly monomeric PMFPs with very good properties have been developed for common SR techniques by our lab and others (Table 1).

The brightness was determined as the product of extinction coefficient and quantum yield.

3.2. *Brightness*

Brighter FPs are always in demand because brightness is a key factor that directly affects the imaging resolution. For all SR imaging methods, brighter fluorescence means that more photons can be collected by the detector and a higher SBR can be achieved. Moreover, brighter FPs require a lower light intensity or shorter acquisition time for the same fluorescence signal, therefore significantly reducing photobleaching and damage to the FPs. Additionally, a shorter acquisition time enables higher temporal resolution. The brightness of a fluorescent protein can be calculated using the formula below:

$$B = \varepsilon_{\lambda ex} \times \Phi_{\lambda ex/\lambda em},$$

where $\varepsilon_{\lambda ex}$ is the molar absorption coefficient at a given excitation wavelength and $\Phi_{\lambda ex/\lambda em}$ is the quantum yield at a given excitation and emission wavelength.

Thus, the photon absorption capability and energy conversion efficiency of a fluorescent protein determine its bulk brightness. However, for single-molecule-based technology such as PALM, the number of photons emitted by a single molecule in one frame, instead of bulk brightness, is what really matters. The photon number is the product of the photon emission rate and the exposure time, and the photon emission rate is proportional to the bulk brightness and incident light intensity. From experience, the brightness of a fluorescent protein for single-molecule imaging should be no less than 3×10^4. For blue and green FPs, this threshold value should be higher, as these proteins may have a higher background signal due to auto-fluorescence.

Table 1. Characteristics of photomodulatable fluorescent proteins.

Proteins	Photo No.	On/off contrast rate ratio	Brightness	Preactivation/postactivation emission wavelength, nm	Maturation time, min	References
			Monomeric fluorescent proteins			
Skylan-S	948	NA	98	511/−	NA	25
PAtagRFP	906	5.7×10^{-6}	NA/5.3	−/595	200	24 and 26
mEos3.2	809	2.6×10^{-6}	53/18	516/580	330	23 and 24
mMaple3	675	6.2×10^{-7}	NA	506/583	49	24
Skylan-NS	669	NA	79	511/−	NA	
PAGFP	313	1.3×10^{-3}	13.7	−/517	<10	24 and 27
Dronpa	262	5.8×10^{-4}	81	−/517	25	24 and 28
			Nonmonomeric fluorescent proteins			
mMaple	798	1.9×10^{-6}	11/17	505/583	48	24 and 29
tdEos	774	3.2×10^{-6}	55/20	516/581	330	24 and 30
mEos2	745	2.9×10^{-6}	47/50	519/584	340	24 and 31
PAmCherry	706	7.8×10^{-6}	NA/8.3	−/595	61	9 and 24
Dendra2	686	4.2×10^{-6}	23/19	507/573	38	24 and 32
mKikGR	599	4.1×10^{-6}	34/18	515/591	31	24 and 33
mGeosM	248	4.9×10^{-4}	NA/44	−/514	<10	24 and 34
PSCFP2	223	8.1×10^{-6}	8.6/11	468/511	NA	24 and 35

3.3. *Photostability*

For SR imaging techniques such as STED and RESOLFT, which use a much higher laser intensity (10^4–10^5 higher than PALM and STORM) than traditional microscopy, the photostability of the FP is one of the indispensable factors that need to be considered. On the other hand, for SR imaging techniques such as PALM and STORM, which need to acquire ten thousand frames to reconstruct one image, high photostability of the FP is also preferable. For a more challenging task such as live cell or 3D SR imaging, the photostability of the candidate FP is the first priority. There are several photostable FPs suitable for 2D super resolution imaging in fixed cells. However, there is still a great shortage of super photostable FPs, especially red and far red FPs, which are useful in 3D and live-cell imaging.

Photostability can be denoted by $\tau_{1/2}$, which is the time required to photobleach half of the maximum fluorescence. The parameter is dependent on illumination conditions, expression systems and fusion proteins; therefore, it is of great importance to measure the photostability in each experiment. Furthermore, note that for RSFPs, which can be turned on/off repeatedly, $\tau_{1/2}$ is the time it takes for the fluorescence maximum of each cycle to decrease to its half value.

3.4. *Maturation time*

With the help of oxygen, newly translated FP peptides go through several chemical reactions that lead to the maturation of the chromophore and to fluoresce. In this process, oxygen acts like a double-edged sword because increased contact of the FPs with oxygen will increase both maturation speed and the risk of bleaching. In most cases, fast maturation means more detectable fluorescent PMFP-fusion molecules at the time of imaging, a higher signal volume, a short acquisition time and, thus, a better time resolution. This is vital for live-cell imaging, which needs to capture nanosecond to second scale movements. Moreover, FPs with short maturation time, such as mEos3.2,[23] will have a higher labeling density, which is a key determinant of the imaging resolution of PALM.[13] Currently, two methods have been introduced to probe the maturation speed of FPs. One method measures the recovery time of denatured FPs *in vitro*, whereas the other directly records time intervals of FP expression and fluorescence *in vivo*. It has been reported that FPs with super folding abilities, such as sfGFP, fluoresce even if their fusion protein is expressed in inclusion bodies.[36] Thus, one can use this method to rapidly determine whether an FP has good folding and maturation properties.

3.5. *Labeling density*

An appropriate labeling density, neither too high nor too low, is the key factor for the higher resolution of both stochastic and patterned subdiffraction excitation SR techniques. A high labeling density provides a high resolution; however, the activating laser power (generally 405 nm) must be optimized to activate separated single molecules at a time for PALM/STORM imaging because more molecules in the off state produce a higher background, and a higher illumination intensity or a longer time is needed to saturate the molecules to the off state for saturation-based SR techniques. Furthermore, a higher labeling density decreases the dynamic fluctuation in SOFI imaging.

4. Optimal Photomodulatable FPs for Different SR Techniques

In addition to the properties mentioned above, other properties of PMFPs, including photons per switching event, on–off duty cycle, contrast ratio and photon conversion efficiency largely dictate the quality of SR images. Different SR techniques require the consideration of different photophysical and biochemical properties. In this review, we discuss the properties of PMFPs that affect their performance in the stochastic or patterned subdiffraction excitation-based SR techniques. Mainly based on our recently developed PCFP and RSFP, we provide important and practical suggestions for choosing PMFPs for most promising live-cell SR techniques, specifically the SOFI and NL-SIM techniques.

4.1. *PMFPs for PALM/FPALM*

In PALM/FPALM imaging, the resolution depends on the localization precision and molecular density. The former describes how well the center of a molecule can be determined, whereas the latter indicates how many molecules can be determined per area unit. Although molecular density has been neglected for a time, it is essential for good PALM imaging. According to the Nyquist criterion, the average distance between two neighboring molecules should be no more than half of the achievable resolution, so a certain labeling density should be achieved. Moreover, the formula of the localization precision below[37] shows that the photon number emitted by a single FP and the contrast ratio of the FP are also important:

$$\langle(\Delta x^2)\rangle = \frac{s^2 + a^2/12}{N} + \frac{8\pi s^4 b^2}{a^2 N^2},$$

where s is the standard deviation of the point spread function, a is the pixel size of the imaging detector, N is the photon number and B is the background noise.

All three types of PMFPs can be applied to PALM imaging. We refer the readers to the recent excellent review of PMFPs for PALM/STORM techniques[8] and Xiaowei Zhuang's research paper.[24] Here, we highlight the important properties of recent PMFPs and present our considerations on their selection for PALM/STORM techniques.

Many PMFPs have been developed for PALM/STORM imaging[8] (Table 1). As mentioned above, the monomeric property is our first consideration for choosing a PMFP. mEos2 is one of the most widely used PCFPs for PALM/STORM microscopy. However, it was found to form dimers and higher-order oligomers at high concentrations.[31,38] We have shown that mEos2 causes incorrect intracellular aggregates when fused to membrane proteins, including G protein–coupled receptor GRM4 and glucose transporter 4 (GLUT4)[23] (Fig. 1). Siyuan Wanga *et al.* also reported that mEos2 exhibits an artificial visible punctum or clusters in *Escherichia coli* when fused to the protease ClpP, nucleoid-associated protein H-NS and Tar protein and causes Vimentin filaments to cluster into thick bundles in mammalian cells.[24] Other PMFPs that have dimerization tendencies and fusion problems include mKikGR, mGeosM, mMaple, PAmCherry, PSCFP2 and tdEos[24] (Table 1). Notably, the authors stated that for those proteins that oligomerize or cluster even without fusion to FPs, even a weak dimerization tendency of FPs may amplify the clustering effect of the target protein and cause artificial clusters.[24] Therefore, because it is not known before the experiment whether the target protein has intrinsic aggregation, PMFPs that are less dimeric or not dimeric, including mEos3.2, Dronpa, PAGFP, mMaple3 and PAtagRFP, as well as our recently developed Skylan-S[25] and Skylan-NS,[22] should be considered first (Table 1).

Next, we consider the photon budget and on/off contrast ratio of PMSFs (Table 1). A higher photon budget leads to higher localization precision and, hence, higher image resolution.[39] Among the

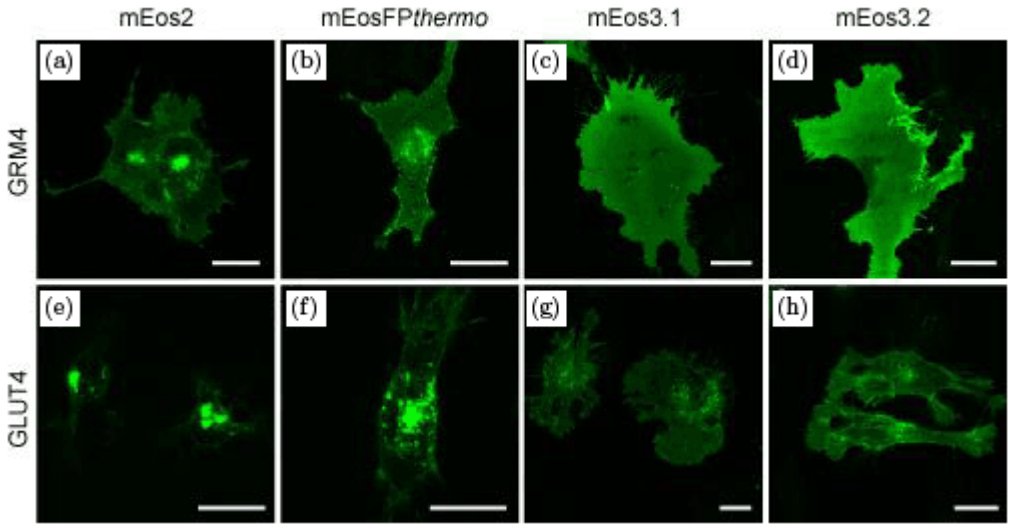

Fig. 1. (a–d) COS-7 cells expressing metabotropic glutamate receptor 4 (also known as GRM4) fused with mEos2 (a), mEosFPthermo (b), mEos3.1 (c) and mEos3.2 (d) were imaged using confocal microscope near the bottom of the membrane. (e–h) GLUT4 (glucose transporter type 4) were labeled with mEos2 (e), mEosFPthermo (f), mEos3.1 (g) and mEos3.2 (h) and transfected into L6 cells. This figure is from Ref. 23.

monomeric PMFPs mentioned above, PAtagRFP and mEos3.2 exhibited the highest photon budgets (800–900) among PAFPs[23,24] (Table 1). The green PAGFP has two-fold fewer photons (200–300) than mEos3.2 and PAtagRFP[24] (Table 1). Slowly switched RSFPs often have higher number of photons per switching event and are thus better suit for PALM. The green RSFPs rsFastLime,[40] rsEGFP[41] and updated version rsEGFP2[42] gave relatively low photon budgets (<60 photons per switching event), which would lead to relatively poor localization precision[24] for PALM/STORM imaging. However, it is worth noting that rsEGFP2 is an excellent alternative choice for RESOLFT due to the large number of switching cycles before photobleaching.[42] Skylan-S is our recently developed RSFP specific for SOFI imaging. However, it can also be used for the PALM/STORM technique at a higher illumination intensity because the photon number before bleaching is high enough.[25]

The on/off contrast ratio is another key property to consider for PALM/STORM imaging (Table 1). For example, Skylan-NS,[22] an RSFP we recently developed specifically for NL-SIM and RESOLFT techniques, has a high single-molecule photon number but is suboptimal for PALM/STORM imaging due to its low single-molecule contrast ratio. The bulk fluorescent signal is much higher than that of other green RSFPs, but it is hard to detect single molecules, possibly because Skylan-NS maturates very fast (unpublished) and can be easily activated to the on state by 488 nm illumination. For PALM/STORM imaging, all the PMFPs are illuminated during imaging, but only one or a few single molecules within the diffraction-limited zone are in the on state and excited to emit photons. However, the abundant other molecules within the diffraction-limited spot and in the off state will produce a high background that affects the detection of the single molecule. The on/off contrast ratio is defined as the ratio of fluorescence between the on state and off state under the illumination of the imaging light only.[43] It is worth noting that the on/off contrast depends highly on the illumination intensity and exposure time, which should be optimized for each PMFP to obtain the optimal single-molecule detection. Because the emission spectrum of activated single molecules is red shifted (compared with that of the inactivated molecules) and detected in a different color channel, PCFPs have much higher contrast ratios than RSFPs and PAFPs and hence better image quality (resolution). Therefore, PCFPs such as mEos3.2 and mMaple3 are the first consideration for PALM/STORM imaging of only one target protein. mEos3.2 has a very high photon budget and can be used for live-cell PALM microscopy using sCMOS camera-specific single-molecule localization algorithms.[44] Compared with mEos3.2, mMaple3 was reported to have higher signal efficiency, which is defined as the ratio

between the number of detectable PMFP-fusion molecules per cell and the expression level of the fusion protein,[24] and thus a higher labeling density and resolution in theory; however, the lower photon budget of single molecules and lower on–off ratio of mMaple3 in the red channel may decrease the spatial resolution in practical use. For RSFPs, the on/off contrast ratio is highly dependent on the labeling density and the activating laser and excitation laser intensities. rsKame is an excellent candidate as a green marker for dual color PALM/STORM.[45] The ideal red partner still needs to be developed, as PAmCherry mentioned above has the problem of dimerization, whereas PAtagRFP has a very low signal efficiency.[24]

The properties discussed above are also suitable for the updated versions of PALM/STORM that image several overlapping single molecules simultaneously.

4.2. *RSFPs for SOFI*

SOFI is a purely calculation-based imaging approach that can produce background- free, contrast-enhanced SR images based on the temporal correlation analysis of fluorescence fluctuation/blinking over hundreds of raw images.[18] In contrast to PALM/STORM imaging, in which only one or several single molecules are stochastically excited, SOFI uses light to stochastically activate small subsets of RSFPs within a densely labeled structure to produce a fluorescence fluctuation. The RSFP properties critical for SOFI imaging include (1) the averaged fluorescence intensity in the fluctuation state, (2) the on/off contrast ratio, (3) the photostability, and (4) the oligomerization tendency. The first three properties determine the fluctuation range of the imaged pixels and the SOFI signal, which are essential to the spatial resolution, and the last may lead to artificial aggregation of the target proteins. As in PALM/STORM imaging, the on/off contrast ratio in SOFI imaging is highly dependent on the labeling density, laser power and exposure time. There are only a few RSFPs reported for SOFI imaging. Dronpa and rsTagRFP could be used for SOFI imaging. However, both have low averaged fluorescence intensity in the fluctuation state, photostability, and on/off contrast ratios, which produce low SOFI signals.[25] Recently, we developed the novel monomeric green RSFP Skylan-S. Compared with Dronpa, Skylan-S has a much higher on/off contrast ratio and photostability[25] (Fig. 2). Notably, Skylan-S exhibits a 4-fold improvement in the fluctuation range of the imaged pixels and an order-of-magnitude increase in averaged fluorescence intensity in the fluctuation state. The higher fluctuation and averaged fluorescence intensity in the fluctuation state of Skylan-S produces a higher second-order cumulant value than that provided by Dronpa at each time point. With Skylan-S, a high resolution SOFI image of live cells can be obtained.

4.3. *RSFPs for RESOLFT/Nonlinear SIM (NL-SIM)*

RESOLFT and NL-SIM belong to the saturated depletion-based SR techniques, which can be implemented by patterned photoactivation of RSFPs to dramatically lower the illumination intensities and decrease the size of the excitation ensemble (point or line). RSFPs can be switched off from a long-lived state under dramatically reduced laser power (nearly one million times lower than the intensity used in STED), which helped the invention of reversible saturable optical fluorescence transitions stimulated emission (RESOLFT). Derived from STED, RESOLFT also uses a donut-shaped beam to switch off, but not deplete, fluorescence in the beam-covered region, and only the molecules at the small center of the beam remain fluorescent; by scanning the small center across the sample, RESOLFT can generate a SR image. Similarly, by replacing the donut-shaped beam with other illumination patterns, such as the sinusoidal stripes used in structured illumination microscopy, and by saturating one of the "on" or "off" states, nonlinear structured illumination microscopy (NL-SIM) increases the imaging speed compared with RESOLFT, and higher resolution than SIM. These two techniques require fewer raw images to reconstruct a final SR structure, making them suitable for live cell imaging.

The following characteristics of RSFPs are most critical for the two SR microscopies: first, the integrated fluorescence signal across each switching cycle, which depends on the absorption cross-section, effective quantum yield and characteristic switching time from the fluorescent "on" to "off" state; second, the fluorescence contrast ratio of the "on/off" states; and third, the photostability under excitation and depletion. As mentioned above, there

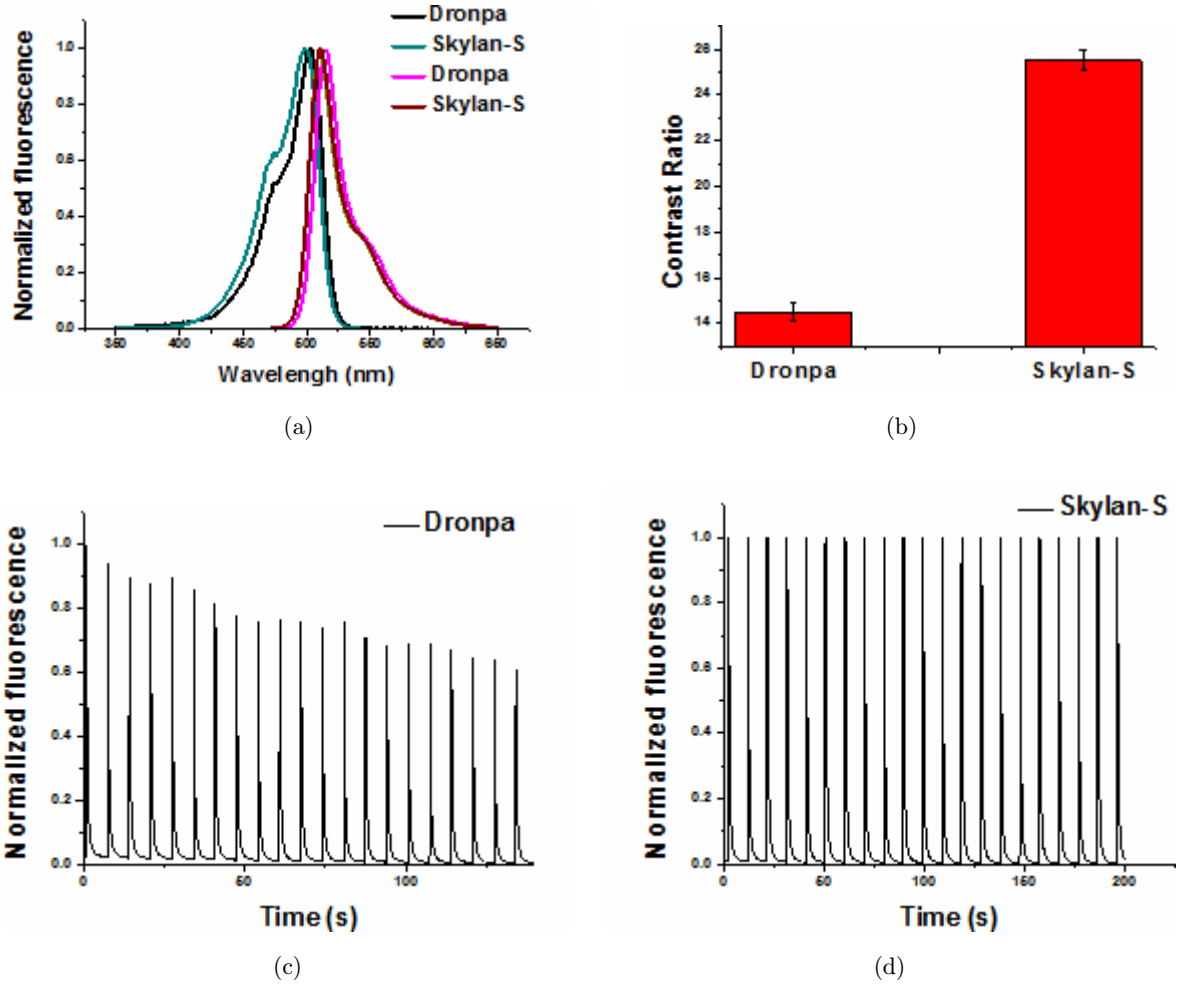

Fig. 2. (a) Excitation and emission spectra (measured at the excitation maximum). The excitation and fluorescence emission spectral profiles of Skylan-S and Dronpa were displayed. (b) Contrast ratios of Dronpa and Skylan-S. (c, d) Photoswitching kinetics of Dronpa and Skylan-S, respectively, measured in *E.coli*. *E.coli* cells expressing Dronpa and Skylan-S were continuously excited with 488 nm illumination (0.24 mW), and pulsed 0.01 s bursts of illumination with 405 nm light at a laser power of 0.2 mW were used to photoactivate the FPs. This figure is from Ref. 25.

are not very many truely monomeric RSFPs with high photon budgets suitable for RESOLFT/NL-SIM imaging. The Dronpa and rsEGFP families have been exploited for the saturated SR imaging. However, Dronpa has a limited number of switching cycles, relatively low fluorescence signal and poor contrast ratio under physiological conditions. Using rsEGFP, Grotjohann *et al.* demonstrated RESOLFT imaging of various living samples at $\sim$40 nm resolution, including bacteria, mammalian cells, and organotypic tissue slices.[41] Additionally, by developing a fast switching mutant rsEGFP2, they increased the pixel dwell time 25- to 250-fold and revealed changes in the ER structure occurring in $<$1 s.[42] rsEGFP2 exhibits extremely high photostability, showing potential utility in time-lapse live-cell imaging. However, the low photon numbers restrict its ability to reach the desired resolution at a reasonable SBR. Currently, we developed a truly monomeric RSFP, Skylan-NS (short for Sky lantern for Nonlinear Structured illumination), with excellent RSFP characteristics for SR live imaging. Skylan-NS produces $\sim$10-fold more photons per switching cycle than rsEGFP2 and a 3.6- or 1.8-fold higher "on/off" contrast ratio than Dronpa or rsEGFP2, respectively. Notably, it provides $\sim$700 switching cycles before bleaching to 1/e of the initial fluorescence intensity. These advantages enable the recently developed technique of patterned activation NL-SIM (PA NL-SIM)[22] live

cell imaging to achieve $\sim$60 nm resolution at sub-second rates with only a 100 W/cm^2 illumination intensity for tens of time points across $40 \times 40\,\mu$m^2 fields-of-view.

5. Future Directions and Challenges: Brighter, Higher Contrast Ratio, and more Colorful

PCFPs have a higher contrast ratio and spatial resolution than RSFPs. However, they occupy two channels, making dual-color PALM imaging either with another PCFP or RSFP (PAFP) a challenge. Although it has been reported that mEos2 can be used with PSCFP2 for dual-color PALM microscopy by sequential imaging of mEos2 and PSCFP2,[46] it is difficult to convert all the green mEos2 to red or bleach all the green mEos2 molecules before acquiring the green signal from the photo-converted PSCFP2. This is also the problem for mEos3. Dendra2 has very high conversion efficiency; however, the single molecule properties are not suitable for PALM imaging (unpublished data). There is an urgent need for PCFPs with high photo-conversion efficiency and excellent single-molecule photons for dual-color PALM/STORM imaging.

Green RSFPs are the best developed ones among RSFPs for both stochastic and patterned-excitation microscopies. In the future, brighter green RSFPs with enhanced contrast ratios and photostability will be required for live-cell SR techniques with higher spatiotemporal resolution and more time points. Additionally, red RSFPs and far-red RSFPs with optimal photochemical characteristics are highly needed for dual color SR imaging.

Acknowledgments

This project was supported by the National Basic Research Program (2013CB910103), the National Natural Science Foundation of China (Grant Nos. 31421002, 31370851 and 31300612), the Project of the Chinese Academy of Sciences (XDB08030202), and the Beijing Natural Science Foundation (7131011). We would also like to acknowledge many investigators whose important work and key contributions could not be cited here owing to space restrictions.

References

1. M. J. Rust, M. Bates, X. Zhuang, "Sub-diffraction-limit imaging by stochastic optical reconstruction microscopy (STORM)," *Nat. Methods* **3**(10), 793–795 (2006).
2. S. T. Hess, T. P. Girirajan, M. D. Mason "Ultra-high resolution imaging by fluorescence photo-activation localization microscopy," *Biophys. J.* **91**(11), 4258–4272 (2006).
3. E. Betzig *et al.*, "Imaging intracellular fluorescent proteins at nanometer resolution," *Science* **313** (5793), 1642–1645 (2006).
4. M. C. Hofmann, S. Eggeling, S. Jakobs, W. Hell, "Breaking the diffraction barrier in fluorescence microscopy at low light intensities by using reversibly photoswitchable proteins," *Proc. Natl. Acad. Sc.i USA* **102**(49), 17565–17569 (2005).
5. M. G. Gustafsson, "Nonlinear structured-illumination microscopy: Wide-field fluorescence imaging with theoretically unlimited resolution," *Proc. Natl. Acad. Sci. USA* **102**(37), 13081–13086 (2005).
6. M. G. Gustafsson, "Surpassing the lateral resolution limit by a factor of two using structured illumination microscopy," *J. Microsc.* **198**(2), 82–87 (2000).
7. S. W. Hell, J. Wichmann, "Breaking the diffraction resolution limit by stimulated emission: Stimulated-emission-depletion fluorescence microscopy," *Opt. Lett.* **19**(11), 780–782 (1994).
8. D. M. Shcherbakova, P. Sengupta, J. Lippincott-Schwartz, W. Verkhusha, "Photocontrollable fluorescent proteins for superresolution imaging," *Ann. Rev. Biophys.* **43**, 303–329 (2014).
9. J. Lippincott-Schwartz, F. V. Subasch *et al.*, "Photoactivatable mCherry for high-resolution two-color fluorescence microscopy," *Nat. Methods* **6**(2), 153–159 (2009).
10. M. Born, E. Wolf, *Principles of Optics: Electromagnetic Theory of Propagation, Interference and Diffraction of Light*, CUP Archive, Cambridge (2000).
11. B. Huang, H. Babcock, X. Zhuang, "Breaking the diffraction barrier: Super-resolution imaging of cells," *Cell* **143**(7), 1047–1058 (2010).
12. S. W. Hell, "Far-field optical nanoscopy," *Science* **316**(5828), 1153–1158 (2007).
13. G. Patterson, M. Davidson, S. Manley, J. Lippincott-Schwartz, "Superresolution imaging using single-molecule localization," *Ann. Rev. Phys. Chem.* **61**, 345–367 (2010).
14. S. J. Holden, S. Uphoff, A. N. Kapanidis, "DAOSTORM: An algorithm for high- density super-resolution microscopy," *Nat. Methods* **8**(4), 279–280 (2011).

15. F. Huang, S. L. Schwartz, J. M. Byars, K. A. Lidke, "Simultaneous multiple-emitter fitting for single molecule super-resolution imaging," *Biomed. Opt. Express* **2**(5), 1377–1393 (2011).
16. T. Quan *et al.*, "High-density localization of active molecules using structured sparse model and Bayesian information criterion," *Opt. Express* **19**(18), 16963–16974 (2011).
17. S. Cox *et al.* "Bayesian localization microscopy reveals nanoscale podosome dynamics," *Nat. Methods* **9**(2), 195–200 (2012).
18. T. Dertinger, R. Colyer, G. Iyer, S. Weiss, J. Enderlein, "Fast, background-free, 3D super-resolution optical fluctuation imaging (SOFI)," *Proc. Natl. Acad. Sci. USA* **106**(52), 22287–22292 (2009).
19. S. W. Hell, M. Kroug, "Ground-state-depletion fluorscence microscopy: A concept for breaking the diffraction resolution limit," *Appl. Phys. B* **60**(5), 495–497 (1995).
20. E. Betzig, A. Lewis, A. Harootunian, M. Isaacson, E. Kratschmer, "Near field scanning optical microscopy (NSOM): Development and biophysical applications," *Biophys. J.* **49**(1), 269 (1986).
21. E. H. Rego *et al.*, "Nonlinear structured-illumination microscopy with a photoswitchable protein reveals cellular structures at 50 nm resolution," *Proc. Natl. Acad. Sci. USA* **109**(3), E135–143 (2012).
22. D. Li *et al.*, "ADVANCED IMAGING. Extended-resolution structured illumination imaging of endocytic and cytoskeletal dynamics," *Science* **349** (6251), aab3500 (2015).
23. M. Zhang *et al.*, "Rational design of true monomeric and bright photoactivatable fluorescent proteins," *Nat. Methods* **9**(7), 727–729 (2012).
24. S. Wang, J. R. Moffitt, G. T. Dempsey, X. S. Xie, X. Zhuang, "Characterization and development of photoactivatable fluorescent proteins for single-molecule-based superresolution imaging," *Proc. Natl. Acad. Sci. USA* **111**(23), 8452–8457 (2014).
25. X. Zhang *et al.*, "Development of a reversibly switchable fluorescent protein for super-resolution optical fluctuation imaging (SOFI)," *ACS Nano* **9**(3), 2659–2667 (2015).
26. F. V. Subach, G. H. Patterson, M. Renz, J. Lippincott-Schwartz, V. V. Verkhusha, "Bright monomeric photoactivatable red fluorescent protein for two-color super-resolution sptPALM of live cells," *J. Am. Chem. Soc.* **132**(18), 6481–6491 (2010).
27. G. H. Patterson, J. Lippincott-Schwartz, "A photoactivatable GFP for selective photolabeling of proteins and cells," *Science* **297**(5588), 1873–1877 (2002).
28. R. Ando, H. Mizuno, A. Miyawaki, "Regulated fast nucleocytoplasmic shuttling observed by reversible protein highlighting," *Science* **306**(5700), 1370–1373 (2004).
29. A. L. McEvoy *et al.*, "mMaple: A photoconvertible fluorescent protein for use in multiple imaging modalities," *Plos One* **7**(12), e51314 (2012).
30. J. Wiedenmann *et al.*, "EosFP, a fluorescent marker protein with UV-inducible green-to-red fluorescence conversion," *Proc. Natl. Acad. Sci. USA* **101**(45), 15905–15910 (2004).
31. S. A. McKinney, C. S. Murphy, K. L. Hazelwood, M. W. Davidson, L. L. Looger, "A bright and photostable photoconvertible fluorescent protein," *Nat. Methods* **6**(2), 131–133 (2009).
32. D. M. Chudakov, S. Lukyanov, K. A. Lukyanov, "Tracking intracellular protein movements using photoswitchable fluorescent proteins PS-CFP2 and Dendra2," *Nat. Protoc.* **2**(8), 2024–2032 (2007).
33. S. Habuchi, H. Tsutsui, A. B. Kochaniak, A. Miyawaki, A. M. van Oijen, "mKikGR, a Monomeric Photoswitchable Fluorescent Protein," *Plos One* **3**(12), e3944 (2008).
34. H. Chang *et al.*, "A unique series of reversibly switchable fluorescent proteins with beneficial properties for various applications," *Proc. Natl. Acad. Sci. USA* **109**(12), 4455–4460 (2012).
35. D. M. Chudakov *et al.*, "Photoswitchable cyan fluorescent protein for protein tracking," *Nat. Biotechnol.* **22**(11), 1435–1439 (2004).
36. K. Solovyov *et al.*, "Expression in E. coli and purification of the fibrillogenic fusion proteins TTR-sfGFP and 2M-sfGFP," *Prep. Biochem. Biotechnol.* **41**(4), 337–349 (2011).
37. K. I. Mortensen, L. S. Churchman, J. A. Spudich, H. Flyvbjerg, "Optimized localization analysis for single-molecule tracking and super-resolution microscopy," *Nat. Methods* **7**(5), 377–381 (2010).
38. H. Hoi *et al.*, "A monomeric photoconvertible fluorescent protein for imaging of dynamic protein localization," *J. Mol. Biol.* **401**(5), 776–791 (2010).
39. R. E. Thompson, D. R. Larson, W. W. Webb, "Precise nanometer localization analysis for individual fluorescent probes," *Biophys. J.* **82**(5), 2775–2783 (2002).
40. A. C. Stiel *et al.*, 1.8 A bright-state structure of the reversibly switchable fluorescent protein Dronpa guides the generation of fast switching variants, *Biochem. J.* **402**(1), 35–42 (2007).
41. T. Grotjohann *et al.*, "Diffraction-unlimited all-optical imaging and writing with a photochromic GFP," *Nature* **478**(7368), 204–208 (2011).
42. T. Grotjohann *et al.*, rsEGFP2 enables fast RESOLFT nanoscopy of living cells, *eLife* **1**, e00248 (2012).
43. G. T. Dempsey, J. C. Vaughan, K. H. Chen, M. Bates, X. Zhuang, "Evaluation of fluorophores for optimal performance in localization-based

super-resolution imaging," *Nat. Methods* **8**(12), 1027–1036 (2011).
44. F. Huang *et al.*, "Video-rate nanoscopy using sCMOS camera-specific single-molecule localization algorithms," *Nat. Methods* **10**(7), 653–658 (2013).
45. A. B. Rosenbloom *et al.*, "Optimized two-color super resolution imaging of Drp1 during mitochondrial fission with a slow-switching Dronpa variant," *Proc. Natl. Acad. Sci.* **111**(36), 13093–13098 (2014).
46. H. Shroff *et al.*, "Dual-color superresolution imaging of genetically expressed probes within individual adhesion complexes," *Proc. Natl. Acad. Sci. USA* **104**(51), 20308–20313 (2007).